

Structure of hydrogen center in D-implanted Si

S. T. Picraux and F. L. Vook

Sandia Laboratories, Albuquerque, New Mexico 87185

(Received 13 April 1978)

Ion-implantation and ion-channeling measurements have been used to study deuterium (D) in silicon. The D was introduced at room temperature by implantation to 13 keV into single-crystal Si. The D was detected and its depth profile was measured by the $D(^3\text{He}, p)^4\text{He}$ nuclear reaction, and simultaneously the Si lattice signal was obtained from the ^3He backscattering. Comparisons of the observed channeling angular distributions with continuum-model calculated distributions for the $\langle 111 \rangle$, $\langle 110 \rangle$, and $\langle 100 \rangle$ axial and $\{110\}$ planar channeling directions indicate that the D is located predominantly in a single interstitial site 1.6 Å along a $\langle 111 \rangle$ direction from a Si atom in the antibonding direction. The resulting structure is compared to other known impurity interstitial centers in Si and implications of this site are discussed.

I. INTRODUCTION

Currently there is great interest in hydrogen in silicon,¹ but only limited direct information is available because of the difficulty of many techniques to detect hydrogen. Although there is more known about defects in Si than any other material, there is no direct information on the structure of hydrogen-related defects in Si. The present work is directed toward this problem and reports the first determination of the lattice location of hydrogen in a semiconductor.

While hydrogen is known to be present in various chemical forms during semiconductor processing, its specific influence on Si device properties has yet to be delineated. Studies have indicated, however, that hydrogen incorporated into silicon-nitride films plays an important role in the charge storage mechanism which in turn controls the memory of metal-nitride-oxide-semiconductor (MNOS) devices.² Also, recently it has been found that hydrogen can be incorporated up to alloy concentrations (1–50 at.%) in amorphous Si films (*a*-Si), greatly altering the electronic and optical properties of *a*-Si.^{1,3} The specific nature of the silicon-hydrogen bonding is not known.

Extrapolation of high-temperature diffusion measurements to lower temperatures suggests that hydrogen should be fairly mobile in crystalline Si at room temperature.⁴ However, studies have demonstrated that hydrogen can be retained relatively immobile for long periods of time in both crystalline⁵ and amorphous⁶ Si at room temperature, suggesting Si-H bonding either with or without defects. A controlled method for the introduction of hydrogen into crystalline Si is by ion implantation. However, the introduction of defects accompanies the implantation process. Ion channeling and electron microscopy have been used to study the damage introduced by hydrogen implantation into Si and results of these studies indicate that there are im-

portant fluence and temperature effects on the behavior of implanted hydrogen in Si.^{7,8} Such effects most likely depend upon the relative concentrations of hydrogen introduced and the relative mobilities of the hydrogen and the defects. The hydrogen location studies presented here are restricted to the low-fluence regime (~0.2 at.%) compared to previous damage studies and we believe this condition to be significant in explaining our results which give a relatively simple site that is interpretable by ion-channeling measurements.⁸

Previous information on the nature of the hydrogen center in crystalline Si has been obtained primarily by optical interactions with vibrational modes. Infrared absorption spectroscopy of implanted H and D isotopes in the low-fluence regime shows that the hydrogen is strongly bonded chemically within the Si lattice, with local mode vibrational spectra characteristic of that observed in silane molecules.⁵ An appreciable number of distinct stretching bands were observed in those studies, but their detailed interpretation in terms of a simple site in association with various defects or in a complex array of sites was not obtained. At higher fluences, infrared absorption and Raman scattering show fewer bands, and these are also characteristic of vibrational modes found for Si-H molecular bonds.⁹ There is also some evidence to suggest that only a single hydrogen atom is involved in the center at low fluences.⁵ Such behavior would be consistent with recent photoelectron emission results for *a*-Si which have been interpreted in terms of Si-H or Si-H₃ bonding at deposition conditions giving, respectively, low or high H concentrations.¹⁰

Previous ion channeling and ion-induced nuclear reaction studies of implanted hydrogen in Si have measured the damage depth distributions⁷ or the hydrogen isotope depth distributions,⁸ but have not given information on the structure of the hydrogen

center in Si. An attempted lattice location measurement for H in Si was mentioned by Ligeon and Guivarch, but they indicated that lower H implant fluences than the $3 \times 10^{16}/\text{cm}^2$ which they used were needed to interpret their data.⁸ Some information is available on the nature of the disorder in hydrogen-implanted Si and its depth distribution, primarily due to the ion channeling and transmission electron microscopy measurements mentioned earlier. These results indicate that the disorder changes appreciably for elevated temperature implants and that microbubbles (presumably containing hydrogen) are formed in elevated temperature implants.⁷ Extremely high-fluence implants have indicated the presence of blisters as observed by scanning electron microscopy.^{8,11}

Relatively little theoretical work has been carried out for hydrogen in bulk Si, although several theoretical studies have been carried out on the nature of hydrogen bonded to the surface of Si. The surface-related calculations have indicated Si-hydrogen bonding to dangling Si bonds for both (100) and (111) surfaces^{12,13} and recently have given evidence for the formation of a chemisorbedlike covalent bond on the (100) surface to second-layer Si without direct interaction with dangling bonds. Calculations for hydrogen in crystalline Si have recently been carried out using extended Hückel theory with and without the presence of vacancies.¹⁴ These calculations have been interpreted in terms of the hydrogen bonded to one of the four dangling Si bonds surrounding a vacancy, or in the absence of vacancies, for a hydrogen atom located in the tetrahedral interstitial site.

The objective of the present study is to better understand the nature of the bonding of hydrogen in crystalline Si through direct measurements of hydrogen lattice location. This system is particularly interesting since more is known about defects and impurities in Si than any other solid, and yet there is no previous experimental information on the structure of the hydrogen center in crystalline Si. Furthermore, a better understanding of the Si-H bond and its structure may bear importantly on the understanding of amorphous Si.

The techniques used here are ion implantation of D into Si, and ion channeling combined with nuclear reaction detection of D and ion backscattering detection of Si, to determine the lattice location of D in Si. We obtain evidence for the existence of a single, well-defined site, which is not currently predicted by theory, for the D center in Si. In Sec. II we describe the experimental techniques used in the present study. Section III summarizes the theoretical calculations of the angular distributions which are used to interpret the experimental results for the D location. The results are presented

in Sec. IV and discussed along with their implications in Sec. V.

II. EXPERIMENTAL TECHNIQUE

Experiments were carried out using intrinsic single-crystal Si, and also P-doped $1\text{-}\Omega\text{ cm}$ Si and B-doped $10\text{-}\Omega\text{ cm}$ Si. No differences in the lattice location results were observed between the different samples. This would be expected since the deuterium concentrations introduced for these studies (~ 0.2 at.%) were several orders of magnitude above the highest doping level. The 13-keV D implants were carried out using a 39-keV D_3^+ beam which was magnetically analyzed and electrostatically swept to obtain laterally uniform implants. All implantations were carried out at room temperature under a vacuum of $\approx 5 \times 10^{-7}$ Torr. The beam was incident at an angle of 45° with respect to the surface normal, with the ion flux typically $\approx 5 \times 10^{12}$ D/cm² sec. The implantation fluence used for the lattice location measurements was 3×10^{15} D/cm². The D depth profile was measured for a fluence approximately one order of magnitude larger. The implantation fluence was determined by charge integration and confirmed by nuclear reaction analysis. Almost all of the implanted D was trapped in the Si crystal. Samples of nonporous anodized Al, which is believed to effectively trap implanted hydrogen except for the small fraction reflected from the target, were used for more accurate calibration of the total D trapping efficiency in Si.

Ion-channeling analysis was carried out at room temperature using ion backscattering to detect the Si atoms at a given depth and nuclear reaction analysis to detect the D by means of the $\text{D}(^3\text{He}, p)^4\text{He}$ reaction. A 700-keV ^3He beam was used with a full width at half maximum (FWHM) beam divergence $\leq 0.06^\circ$. The angular resolution of the goniometer was $\leq 0.01^\circ$. A 300-mm² detector was covered with an aluminized mylar foil to stop the backscattered ^3He particles except for several holes in the foil which were introduced to allow the backscattering signal from the Si to be monitored simultaneously and at approximately the same signal strength as the proton signal from the nuclear reaction with D. The angle of detection was at $\approx 135^\circ$ and the detector solid angle was ≈ 0.2 sr. The ^3He backscattered signal from the Si was energy analyzed so that the Si signal corresponded to the same depth region in which the implanted D depth profile occurred. Channeling analysis was carried out along the $\langle 100 \rangle$, $\langle 111 \rangle$, and $\langle 110 \rangle$ axial directions and the $\{110\}$, $\{111\}$, and $\{100\}$ planar directions with the analysis fluence per point ranging from 4 to 7 μC for an analysis beam area ≈ 1 mm².

The deuterium depth profile was determined with a second detector using the same nuclear reaction $D(^3\text{He}, \alpha)\text{H}$ by energy analysis of the emitted α particles. The emitted energy profile was converted into the deuterium depth profile through a knowledge of the particle energy-loss rates and reaction kinematics. An uncovered detector with a vertical slit to limit the spread in detection angle to $<1^\circ$ was placed at $\theta_{\text{lab}} = 77^\circ$. The incident ^3He beam was at an angle of 29.5° with respect to the surface normal resulting in the emitted α particles being at a glancing angle of $\theta_g = 16.5^\circ$ with respect to the Si surface. The relative differential cross section vs energy for the $D(^3\text{He}, \alpha)\text{H}$ reaction was determined experimentally in the same system using a 3-keV D-implanted Si target with correction for the mean depth of the D below the surface. The absolute value was calibrated relative to measurements of Ref. 15. The θ_g was determined to a precision of better than 1° by means of a backscattering analysis of a 1000-Å-thick Au film as a function tilt angle.

The α particles are emitted at energies ~ 3.9 MeV and their yield $dY(E_3)$ in detected energy interval dE_3 is related to the deuterium concentration in atomic fraction C_D by

$$C_D = \frac{dY(E_3)}{dx} \frac{\cos\theta_1}{\phi(d\sigma/d\Omega)_{\text{lab}}(d\Omega)_{\text{exp}}}, \quad (1)$$

where ϕ is the number of incident ^3He particles, $(d\sigma/d\Omega)_{\text{lab}}$ the reaction differential cross section converted to lab coordinates and $(d\Omega)_{\text{exp}}$ the experimental solid angle of detection. The detected solid angle was determined from 2-MeV ^4He and 700-keV ^3He scattering from Si assuming Rutherford values for the elastic scattering cross section.

The depth scale dx in atoms/cm² is related to the detected particle energy scale by

$$dx = \left[-dE_3 / \left(\frac{\epsilon_a(E_1)}{\cos\theta_1} \frac{\partial f(E_1)}{\partial E_1} + \frac{\epsilon_b(E_2)}{\cos\theta_2} \right) \right] \frac{\epsilon_b(E_2)}{\epsilon_b(E_3)}, \quad (2)$$

where ϵ_a and ϵ_b are the stopping powers in the target for incident particle a and emitted particle b , E_1 is the energy of the incident particle at depth x before the reaction, E_2 the energy of the emitted particle at depth x , E_3 the detected energy of the emitted particle after passing back out of the target and $f(E_1) = E_2$. The depth dx is converted from atoms/cm² to depth in cm by dividing by the atomic density of the target, and in this case the value for crystalline Si of 5.00×10^{22} /cm³ was used. The above equations assume $\partial E_2/\partial E_3$ at depth x is $\approx [\epsilon_b(E_2)/\epsilon_b(E_3)]$ which is a very accurate assumption here since the deuterium does not contribute apprec-

ably to the total stopping power of the target.

The depth resolution in the D profile measurement was ≈ 225 Å and was limited primarily by the combination of the angular acceptance of the detector due to the reaction kinematics and the energy resolution of the detector. The absolute depth scale is estimated to be accurate to $\pm 10\%$, and is determined by the experimentally used electronic stopping power for the incident and emitted particles and also by the accuracy with which the angle between emitted α and the Si surface is determined.

III. ANALYTIC TECHNIQUE FOR CHANNELING ANGULAR DISTRIBUTIONS

The location of D in the Si lattice is determined by comparison of the experimentally measured angular distributions to the theoretical distributions calculated as a function of assumed D site.¹⁶ The calculated distributions are a composite of all equivalent projected positions of the impurity along a given channel, as given by the symmetry of the system. The interpreted site is that which gives the best overall agreement between calculations and measurements for all the various axial and planar channeling directions studied.

The calculations are based on the continuum model to obtain the spatial channel particle density as a function of incident angle. Multiple-scattering effects by the electrons and the thermally vibrating lattice atoms have not been included in the present calculations. However, the thermal vibration of the D atoms is accounted for by assuming a Gaussian spatial distribution for the D atoms about their equilibrium site. An rms vibrational amplitude of 0.2 Å was assumed. For axial channeling, the flux density of particles at any position \vec{r} within the channel is given by

$$\rho_{\text{axial}}(r, \psi_0) = \int \frac{d\vec{A}(r_0)}{A(E_1)}, \quad (3)$$

$$E_1 = E\psi_0^2 + U(\vec{r}_0) \geq U(\vec{r}),$$

where E the incident energy, U the continuum potential, E_1 the energy corresponding to the transverse momentum of a particle entering the channel at position \vec{r}_0 with angle ψ_0 with respect to the axis, and A the area available to a particle with a given value of E_1 . Equation (3) is solved numerically by computer code. The spatial probability distribution about the D site due to thermal vibration is given by

$$dp = e^{-r^2/\rho^2} d(r^2/\rho^2). \quad (4)$$

The corresponding flux density for planar channeling at a distance x from the channel center is given by

$$\rho_{\text{planar}}(x, \psi_0) = 4E^{1/2} \int \frac{dx_0}{\lambda[E_1 - V(x)]^{1/2} + f_r}, \quad (5)$$

$$V(x) \leq E_1 \leq E_c,$$

where $E_1 = E\psi_0^2 + V(x_0)$; $x_0 > 0$; $x, x_0 = 0$ corresponds to the channel center; E_c is the critical transverse energy for channeling, f_r is the random fraction, V is the planar continuum potential, and λ is the wavelength of a channeled particle with transverse energy E_1 . The planar calculational method has been described in detail previously.¹⁷

Once a particular trial site for the impurity is selected, its projected position in the channel for all equivalent locations must be determined. One way to do this for these statistical equilibrium calculations is to take a given site and determine the projected position in all equivalent channels, i.e., for the $\langle 111 \rangle$ axial direction this would correspond to the four axes $[111]$, $[\bar{1}\bar{1}1]$, $[1\bar{1}\bar{1}]$, and $[\bar{1}\bar{1}\bar{1}]$.

IV. RESULTS

To measure the D depth distribution accurately, one implant was carried out to a fluence of 2.5×10^{16} D/cm², approximately one order of magnitude greater than that used in the lattice location studies. In Fig. 1 is shown the D depth profile for a 45° incident 13-keV D implant as determined by energy analysis of the emitted α particles from the nuclear reaction $D(^3\text{He}, \alpha)\text{H}$. The experimental depth profile is compared to the theoretically calculated profile¹⁸ for the D distribution. The calcu-

lation uses a coefficient $k = 1.55k_{L\text{indhard}}$, for the electronic stopping power $S_e = kE^{1/2}$, which was determined experimentally for H in Si by comparing low-temperature damage profiles with Monte Carlo calculations of damage energy deposition distributions.¹⁹ In addition, the theoretical damage deposition profile of the implanted D was calculated by the Brice theory¹⁸ for the same electronic stopping cross section and is shown in Fig. 1 for comparison. Both theory and experiment in Fig. 1 correspond to D ions incident at an angle of 45° with respect to the surface normal.

Our measured D profile is in good agreement with that theoretically calculated based on the above electronic stopping cross section. The increased concentration at the deeper depths and decreased concentration at the peak in the distribution may be due in part to channeling of some of the incident D. The D depth distribution is seen to be consistent with the D atoms remaining approximately at their end of range after implantation in crystalline silicon. The maximum D concentration is ≈ 2 at.% for this high-fluence implant and thus in all the lattice location measurements the implant conditions correspond to a local D concentration ≤ 0.2 at.%.

Experimental results for the channeling angular distributions are given in Fig. 2 for three major channeling directions. The implanted D fluence in these and subsequent measurements is 3×10^{15} /cm². The triangles indicate the yield from the D due to the nuclear reaction and the circles the

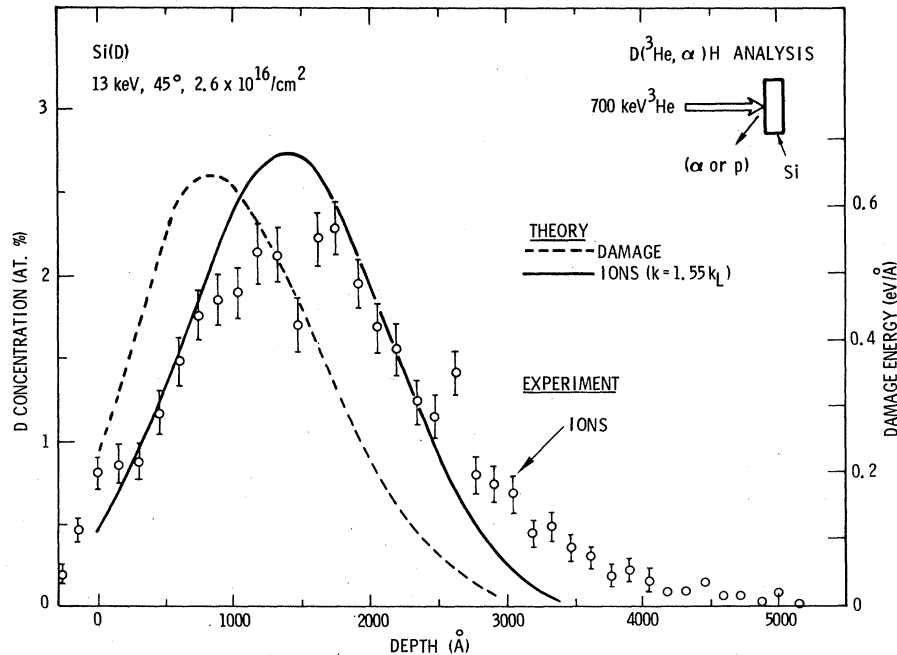


FIG. 1. Measured and calculated D depth profile for a factor of 10 higher fluence implant than used in the lattice location measurements. Measured profile is determined by energy analysis of emitted α particles using the $D(^3\text{He}, \alpha)\text{H}$ reaction. Also shown by the dashed line is the calculated damage deposition profile.

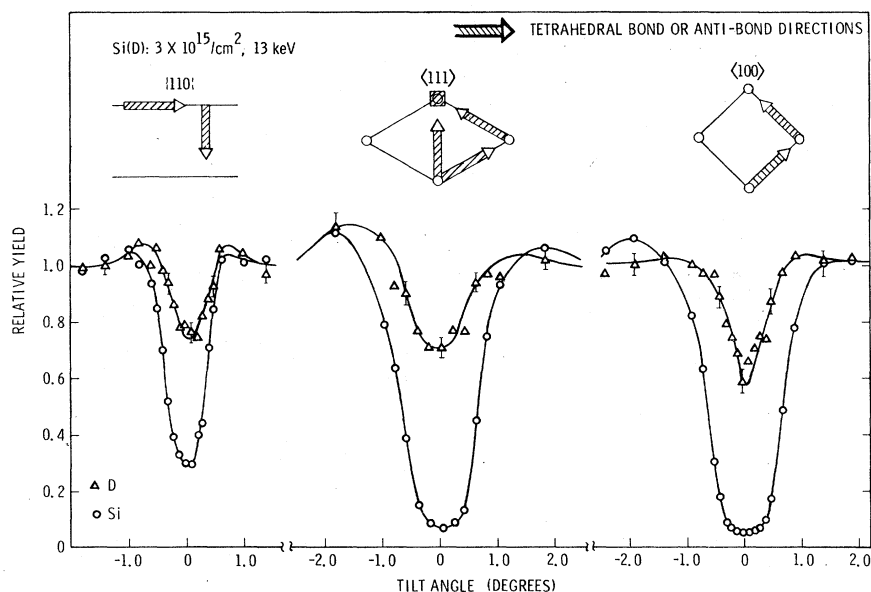


FIG. 2. Measured angular distributions for D (Δ) and Si lattice atoms (\circ) for the $\{110\}$, $\langle 111 \rangle$, and $\langle 100 \rangle$ directions. Insets show by the arrows the projected position of the D site as a function of distance from a Si atom along the $\langle 111 \rangle$ direction where the lines correspond to the planes and the circles to the rows.

yield from the Si due to ion backscattering. The two yields are obtained simultaneously. The D data shown in Fig. 2 indicate well-defined dips along the three channeling directions, the $\{110\}$ plane, $\langle 111 \rangle$ axis, and $\langle 100 \rangle$ axis. Also along the $\langle 100 \rangle$ direction the D dip is appreciably narrowed relative to that for the Si. The presence of these dips for the D signal indicates that the D occupies a nonrandom location relative to the Si lattice.

The $\langle 111 \rangle$ rows contain the Si-Si bonds in the tetrahedrally coordinated Si lattice and the data of Fig. 2 are consistent with the D located along the $\langle 111 \rangle$ direction. This is seen by referring to the insets in the upper part of the figure where the arrows originate from a lattice position and move in $\langle 111 \rangle$ directions. For the three directions given in Fig. 2, the observed results would be the same whether the D position were displaced either along a $\langle 111 \rangle$ direction towards the nearest-neighbor Si atom (referred to as a bond direction) or in the opposite direction towards the tetrahedral interstitial hole (referred to as the antibond direction).

For the $\{110\}$ plane, a site located anywhere along the $\langle 111 \rangle$ direction is always 50% shielded within the $\{110\}$ planes and the other 50% of the projected positions move across the $\{110\}$ channel with increasing distance from a Si atom (see arrows in Fig. 2). Thus, one would expect an approximate 50% dip with an equal or weaker contribution which could range anywhere from a narrowed dip to a central flux peak superimposed on this dip. The observed experimental signal is seen to be a dip of the order of 50% indicating the D is located along this direction and at a distance which

places the interstitial component of the site intermediate between the center of the channel and the $\{110\}$ planes.

Correspondingly for the case of the $\langle 111 \rangle$ axis shown in the center panel of Fig. 2, movement of the D along the $\langle 111 \rangle$ directions from a Si atom maintains one quarter of the available sites along a $\langle 111 \rangle$ row with the others moving towards adjacent rows, as indicated in the upper part of the figure. For distances along the $\langle 111 \rangle$ direction consistent with that indicated by the $\{110\}$ planar data this would result in the D atoms being sufficiently close to the $\langle 111 \rangle$ rows and removed from the center of the channel to not give strong flux peaking effects in the D signal, and rather to contribute slightly to an additional reduction of the $\langle 111 \rangle$ yield from the 25% of the sites which lie directly along the $\langle 111 \rangle$ row along which the channeling is being measured. This is consistent with the experimental results shown in Fig. 2 where the $\langle 111 \rangle$ dip is $\approx 32\%$ of the Si dip.

Finally, for the $\langle 100 \rangle$ direction shown in the right-hand side of Fig. 2, the sites along the $\langle 111 \rangle$ direction at distances approximately consistent with those anticipated from the $\{110\}$ planar and $\langle 111 \rangle$ axial data are such that the sites would lie relatively close to the adjacent $\langle 100 \rangle$ rows and therefore would be expected to give rise to a narrow dip. This is found experimentally as is seen in Fig. 2.

Since the qualitative interpretation of the channeling data for D implanted in Si as shown in Fig. 2 is consistent with the D being located along the $\langle 111 \rangle$ directions, we consider likely possible sites

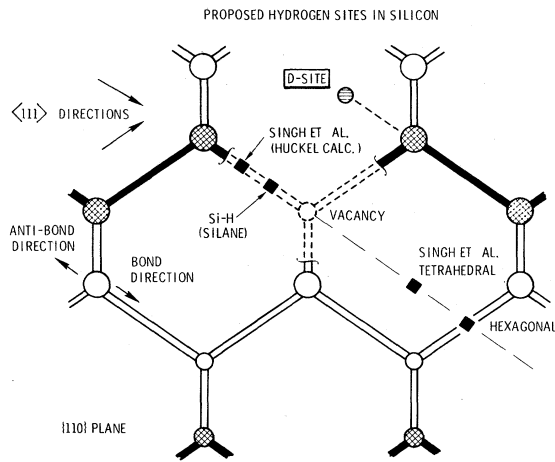


FIG. 3. View of the $\{110\}$ plane in the Si lattice with proposed hydrogen sites and our interpreted site shown.

along $\langle 111 \rangle$ directions. In Fig. 3, the cross-hatched circles correspond to Si atoms in a $\{110\}$ plane of Si and the large open circles to Si atoms in planes directly above and below the plane of the paper. The tetrahedral bonds are indicated by the lines between the atoms and the shaded bonds indicate $\langle 111 \rangle$ directions within the plane of the paper. Also the bond and antibond directions from a Si atom, which correspond, respectively, to $\langle 111 \rangle$ directions towards and away from the nearest-neighbor Si atoms, are indicated in the figure.

Several proposed and theoretically predicted sites for the location of hydrogen in Si are shown in Fig. 3. Also shown is the D site which we find in the present experimental study. Using extended Hückel theory, Singh *et al.*¹⁴ have predicted that the tetrahedral interstitial site is occupied by hydrogen in the absence of defects and a site along the bond direction 0.81 \AA from a Si atom towards a vacant lattice site is occupied by hydrogen in the presence of a vacancy or divacancy. Other sites which might be reasonable to propose for hydrogen in the silicon lattice would include the hydrogen located along a bond direction $\approx 1.47 \text{ \AA}$ from a Si atom towards a vacancy. This bond distance corresponds to that for SiH and Si-D bonds in the silane (SiH_4 or SiD_4) molecule. In general, the Si-hydrogen isotope bond distances are close to 1.47 \AA in almost all molecules containing hydrogen and Si in which the Si has a +4 valence.²⁰ Such a site would seem consistent with current suggestions that hydrogen saturates dangling bonds in amorphous Si films. Still another high-symmetry pure interstitial site is the hexagonal interstitial site in silicon, which is also shown in Fig. 3.

It should be noted that all the proposed sites for

the hydrogen location in Fig. 3 lie along a $\langle 111 \rangle$ direction from Si lattice sites. This serves to further motivate the qualitative discussion of Fig. 2 where it will be recalled that the experimental data suggested that implanted D in Si is located approximately along $\langle 111 \rangle$ directions from Si lattice sites. Furthermore, it should be noted in Fig. 3 that for appropriate channeling directions appreciable differences in the signal would be expected for D located at reasonable bond distances from Si atoms along either the bond or antibond directions. In particular, the $\langle 110 \rangle$ axis is normal to the plane of the paper in Fig. 3 and here it is seen that D locations along antibond directions correspond to the D in the central region of the $\langle 110 \rangle$ channel while for locations along bond directions the D remains along a boundary region of the channel. The former would be expected to give rise to flux peaking and the latter would not.

To first determine whether the D lies along bond or antibond directions the results for the $\langle 110 \rangle$ axis are shown in Fig. 4. The experimental data clearly indicate an enhancement in the yield (flux peak) from deuterium along the $\langle 110 \rangle$ axis. Also shown are the calculated angular distributions for the D located a distance 1.6 \AA from the Si atom in the bond and in the antibond directions. This distance in the antibond direction, as will be discussed later, gave the best overall agreement with our data. The data are clearly observed to disagree with the deuterium located in the bond direction; whereas, the calculation for the 1.6 \AA antibond displacement gives moderately good agreement with the experimental observation.

The theoretically calculated flux peaks would be expected to be somewhat sharper and greater in magnitude than those experimentally observed since the calculations neglect multiple scattering due to the electrons and thermally vibrating lattice atoms. Since the experimental measurements are made at finite depth, these effects would be expected to increase the transverse energy of channeled particles and give a reduction in the flux peak and smoothing of the structure. Also given in Fig. 4 are our calculated angular distributions for the D sites neighboring vacancies or divacancies as theoretically predicted by Singh *et al.*¹⁴ The relatively small bond distance of 0.81 \AA in this case gives rise to a strong dip in the D signal for both bond and antibond displacements, and therefore disagrees with experimental observations in either case.

Channeling along the $\langle 111 \rangle$ axis should be quite sensitive to the presence of D in or near the tetrahedral interstitial site, since for this case the D signal should coincide with that for the Si lattice. As seen in Fig. 5, the experimental D distribution

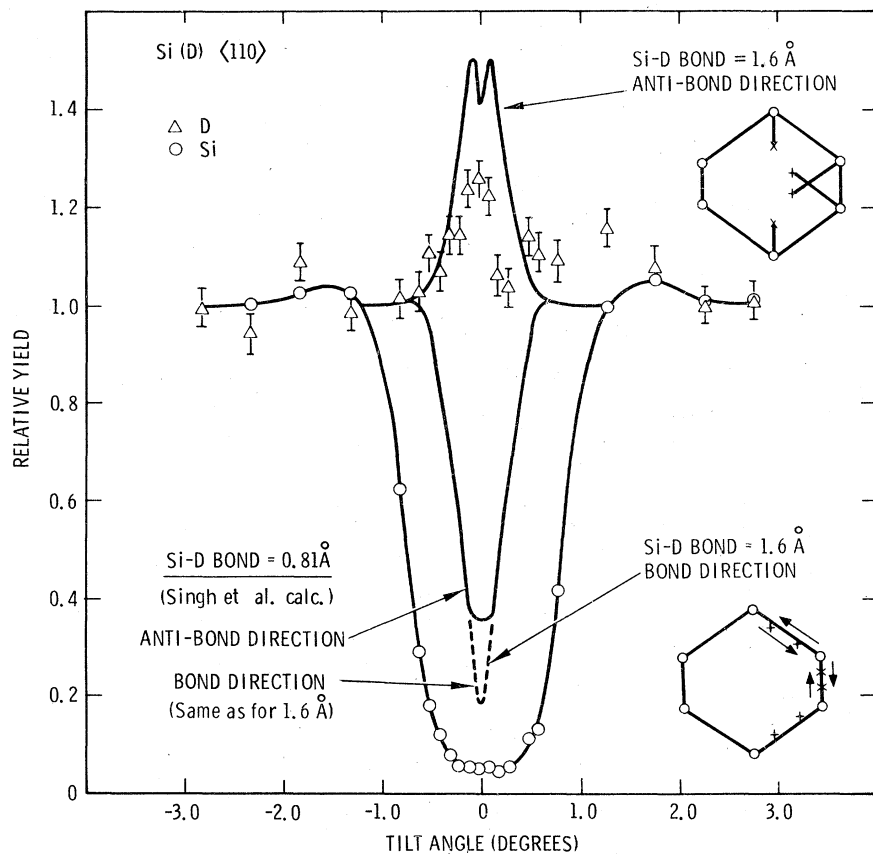


FIG. 4. The $\langle 110 \rangle$ axial angular distribution as observed and as calculated for the indicated sites. The triangles correspond to the D atom signal and the circles to the Si lattice atoms. Insets show projected positions of D by crosses for the 1.6 Å bond and anti-bond sites.

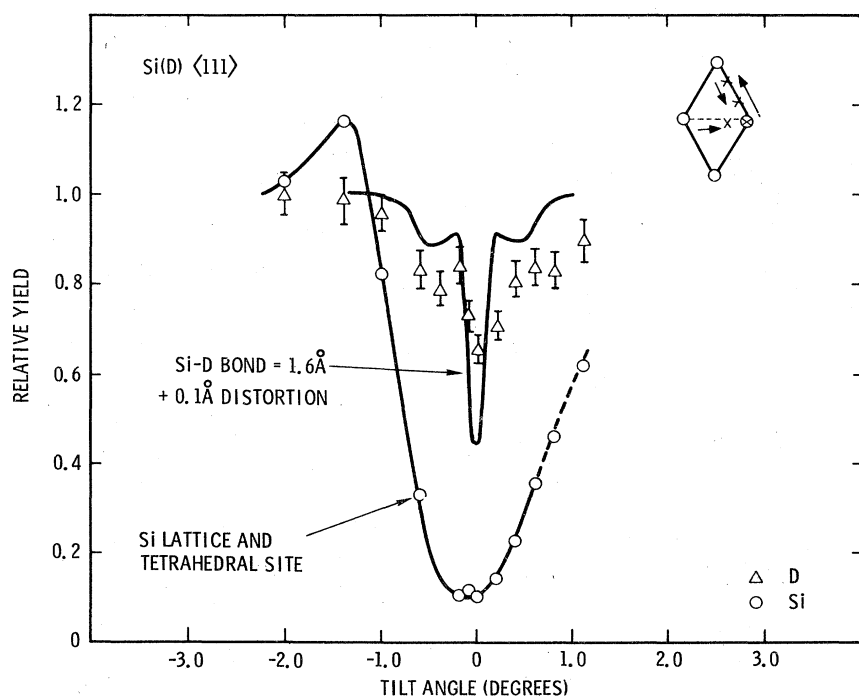


FIG. 5. The $\langle 111 \rangle$ axial angular distributions as observed and as calculated for the 1.6 Å and the tetrahedral site. Inset shows projected positions for 1.6-Å site.

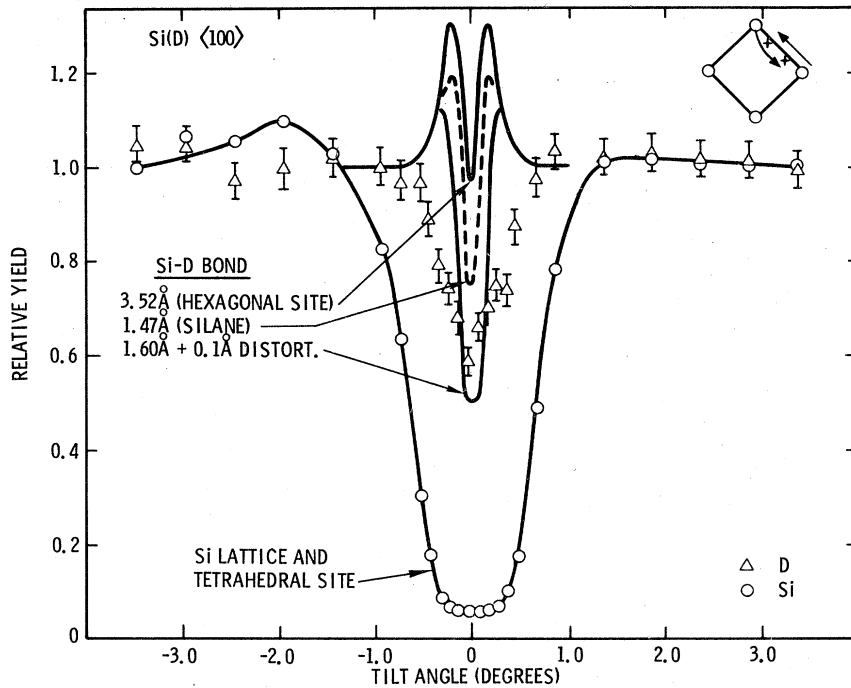


FIG. 6. The $\langle 100 \rangle$ axial angular distributions as observed and as calculated for the indicated sites. Sites are all along a $\langle 111 \rangle$ direction and the projected positions are indicated schematically by the inset.

shows a small dip but is distinctly different from that which would be expected for tetrahedral site occupancy. The theoretically calculated distribution for the best single site which we conclude for the D location in this study is given by the indicated solid line. This corresponds to a D distance of 1.6 Å from a Si lattice site with a small distortion of 0.1 Å transverse to the $\langle 111 \rangle$ direction. This small distortion does not have a noticeable effect on the calculated $\langle 110 \rangle$ distributions shown in Fig. 4. The lattice symmetry is such that the projected D sites are the same for the $\langle 111 \rangle$ channels whether the D is in a bond or antibond direction from Si lattice sites.

As indicated earlier, a dip is found for the D signal along the $\langle 100 \rangle$ axial direction and this dip is narrowed relative to that for the Si lattice. The degree of narrowing and magnitude of the dip should be sensitive to the displacement distance along the $\langle 111 \rangle$ direction and would be the same for displacements either along the bond or antibond directions. The $\langle 100 \rangle$ experimental results are shown in Fig. 6 together with calculations for four different sites, all of which lie along the $\langle 111 \rangle$ direction but at different distances from Si sites. The $\langle 100 \rangle$ angular distribution expected for the tetrahedral interstitial site again coincides with that for the lattice and is clearly seen to disagree with the experimental data. Calculations shown for other possible sites include the hexagonal interstitial site, the silane

site, and our interpreted site which lies 1.6 Å from a Si site. For these cases projections along the $\langle 100 \rangle$ direction correspond to distances of 0.95, 0.71, and 0.60 Å from the nearest $\langle 100 \rangle$ row for the hexagonal, silane and 1.6 Å site, respectively. The calculated angular distributions show a transition from a multiple flux peak to a narrowed dip as the D site moves closer to $\langle 100 \rangle$ rows in this progression. The hexagonal site is clearly seen to disagree with the experimental data and the 1.6 Å displacement gives appreciably better agreement than the silane bond distance. The shoulders or small peaks to either side of the narrow dip for the 1.6 Å calculation are rather sensitive to the approximations of statistical equilibrium, no multiple scattering, and the continuum model, and therefore the results are believed to give fairly reasonable agreement with experimental data. The comparison certainly eliminates the hexagonal and tetrahedral sites and suggests that the bond distance is greater than that of ≈ 1.47 Å for the silane bond, and at least of the order of 1.6 Å.

In Fig. 7 is shown the experimental results for the $\{110\}$ plane which also shows a distinct dip. Again, the D dip would have to coincide with the Si lattice dip if the tetrahedral site were occupied, and this is clearly not the case. Comparison of the calculations for the 1.6 Å distant interpreted site with the experimental data gives good agreement (see dashed line in Fig. 7). In addition when

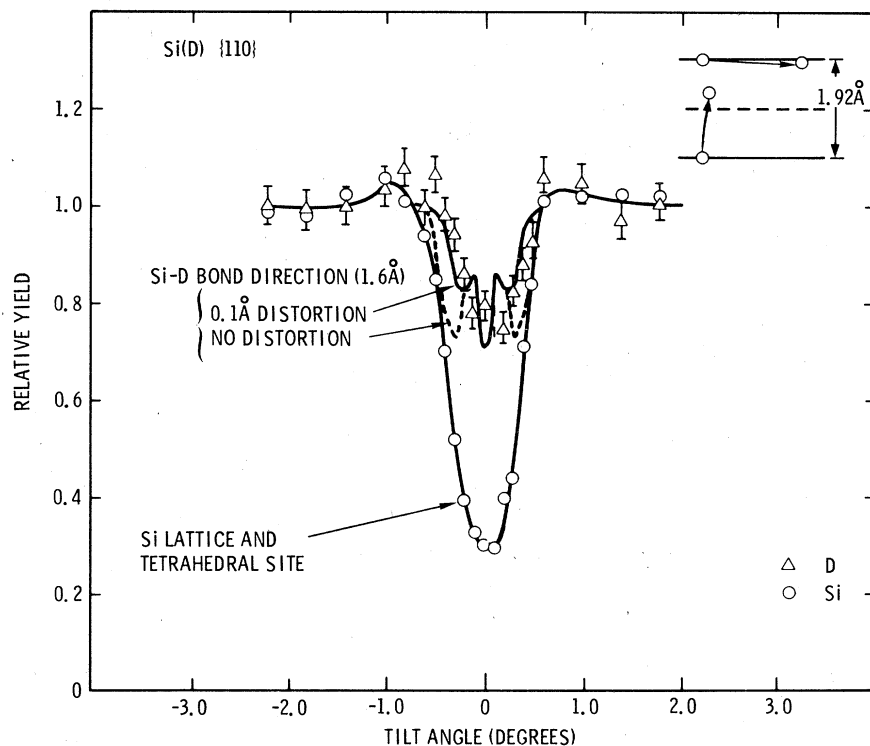


FIG. 7. The $\{110\}$ planar angular distribution as observed and as calculated for the 1.6-Å Si-D bond distance with and without 0.1-Å distortion. Inset indicates D positions by circles with distortion included.

the small distortion of 0.1 Å transverse to the $\langle 110 \rangle$ direction in the $\{110\}$ plane is included, as given by the solid line, a further improvement in agreement results. The fine structure in the dip is not expected to be resolved in the experimental measurements due to multiple scattering effects; however, the envelope of the dip is appreciably narrowed by the distortion due to the movement of $\frac{1}{2}$ of the projected D sites lying in the $\{110\}$ planes out of the planes. It is this narrowing seen in the experimental data which suggests the possibility of the distortion. Experimental angular distribution measurements were also taken for the $\{100\}$ and $\{111\}$ planar directions. These channeling directions are relatively weak, and the D signal showed no resolvable orientational effects for the $\{100\}$ direction and only a weak flux peak for the $\{111\}$ direction. In neither case did the angular distribution contribute substantially to the interpretation of the D lattice site.

V. DISCUSSION

Extrapolation of high-temperature diffusion data⁴ to room temperature suggests that hydrogen and deuterium should be mobile in Si at room temperature. However, the present studies were carried out at room temperature and indicate almost all the implanted D was trapped. In addition, the

close correspondence between the experimental and theoretical depth profiles for the implanted D (Fig. 1) indicates that either physical or chemical trapping of the deuterium occurs very near the end of range. Confidence in the accuracy of the theoretical profile is given by the fact that an experimentally measured electronic stopping power was used in the calculation. In Fig. 1, the D trapping near the end of range indicates the D does not diffuse forward to decorate the damage production profile shown by the dashed line. This could be due either to D trapping in the absence of defects by chemisorption-type bonding into the Si tetrahedral structure or by sufficient defects in the tail of the damage distribution or sufficient total number of defects and defect mobility to trap essentially all the D atoms before they are able to undergo appreciable migration. Using the total damage energy¹⁸ and a Kinchin-Pease description we estimate that approximately 20 interstitial-vacancy pairs should be created for each incident D ion at these implant energies. Since this may provide sufficient damage to trap all the D near their end of range, we are unable to determine in the present measurements whether or not the D is associated with a vacancy or other defect.

Infrared (ir) absorption measurements of the local mode stretching vibrations for H and D im-

planted into Si at similar and higher energies clearly demonstrate the chemicallike bonding of hydrogen to Si lattice atoms.⁵ This interpretation is based on the similarity of the observed ir absorption bands to those for silane molecular bonds. Also mixed H and D implantations suggest that only single hydrogen atoms are involved in the center.

The D concentrations, which in our implanted samples for the location measurements were a factor of 10 less than for the depth profile measurement of Fig. 1, correspond to ~ 0.2 at.% at the maximum of the D depth profile and indicate a high density of available sites. Further evidence for the existence of sufficient trapping sites for all the D is given by the fact that the D profile follows the end-of-range profile even at an order of magnitude higher implant concentration. Also within a resolution of $\pm 10\%$ nearly all the implanted D was trapped within the Si lattice, based on our calibration implants done at the same time in hard anodized Al_2O_3 films.

A relatively large number of bands is observed by ir spectroscopy⁵ and suggests the possibility either of a complex of sites for the D atoms or a relatively simple projected D location with sufficient perturbations in surrounding nearest-neighbor Si atoms to give rise to the various observed bands. These alternatives cannot be distinguished by ion channeling measurements since the surrounding lattice symmetry is not measured by the channeling technique but only the projected position of the impurity atom being studied. The latter interpretation may suggest that the hydrogen is located in association with Si lattice defects. The association of the H with defects is also suggested by the observation of Stein⁵ that after some of the H-implantation-induced ir bands are annealed, subsequent room temperature Ne implantation regenerates the bands. Finally, it is interesting to note that H and D implantation in Si to extremely high fluences results in appreciably fewer ir bands,⁹ suggesting some limiting single type of Si-H band is formed.

Several conclusions about the nature of the D center in Si can be drawn from the present lattice location measurements. It has been found that a single site for the D atoms gives moderately good agreement between theoretically calculated angular distributions and those experimentally observed. Also, this site lies along $\langle 111 \rangle$ directions relative to the Si lattice atoms. Because of the tetrahedral coordination of Si lattice atoms along $\langle 111 \rangle$ directions, this suggests that the D bond to Si may be strongly chemical in nature. Although the major open interstitial sites in the Si lattice lie along this direction these sites are not occu-

ried. In general, less structure is observed in the experimental angular distributions than in the calculated distributions and this would be expected in part from the approximations in the lattice continuum model channeling calculations used here. However, the differences also may reflect some distortional variation of the order of a few tenths of an angstrom in the D sites. Also, the D atom vibrational amplitude should be ~ 0.2 Å, and these two factors taken together limit the accuracy to which the D can be localized in a meaningful way in the present experiments. Taking all the experimental data together the best overall agreement is obtained for the D being located along a $\langle 111 \rangle$ direction a distance 1.6 Å from the Si lattice site in the antibond direction with some small transverse distortion present of the order of 0.1 Å.

Relatively little theoretical work has been carried out on the location and nature of hydrogen centers within bulk Si, although there is much current interest in these questions, particularly in the area of hydrogenated amorphous Si films. One theoretical calculation using extended Hückel theory methods has been used for H in single crystal Si.¹⁴ Results of this calculation gave an energetically stable position for the hydrogen atoms in the tetrahedral interstitial site in the perfect lattice. In the presence of a vacancy or divacancy a different site was obtained, with the D at the end of dangling Si bonds a distance of 0.81 Å in a bond direction towards the position of the vacancy. More recently, based on the present results, these authors have also considered antibond positions and find local minima in the system energy for these directions when a vacancy is present, but at appreciably higher energy levels than for the bond directions.²¹ Again the calculated bond distances for the bond and antibond positions are similar. All these sites are in disagreement with and cannot account for the present experimental observations.

Since extended Hückel theory calculations tend to underestimate nuclear repulsions, it may be that the Si-H bond distance would be increased if this term had been more accurately included in the above calculations. However, it is quite interesting to note that a local minima was predicted in the antibond direction. The authors did emphasize that due to the approximate nature of extended Hückel theory calculations the results may be semiquantitative rather than exact in nature. It would be quite interesting in such calculations to examine whether Si interstitial complexes in association with hydrogen atoms would also be stable.

Fairly extensive theoretical work has been carried out recently for the case of hydrogen on the

surface of Si.^{12,13} These results, as well as surface experiments,²² all tend to suggest that the hydrogen can attach to dangling Si bonds. In the case of the {111} surface, experimental²³ and theoretical¹³ studies further suggest that a trihydride-type surface structure may be formed by the removal of the atomic layer of Si. Recently, calculations have suggested that a covalentlike chemisorption bond of appreciable energy also forms in the case of the {100} surface.¹² This bond has appreciable binding energy (≈ 1 eV) and the D atom is found to locate between and slightly above the two surface Si atoms and directly over a second layer Si atom. While such surface structures should not be directly extendable to bulk configurations, the results do suggest the possibility at sufficiently low temperatures of direct chemical bonding of hydrogen into the Si lattice in the absence of lattice defects.

More is known about point defect and impurity centers in crystalline silicon than in any other solid. Thus, it is particularly interesting to compare our information about the structure of the D interstitial impurity center in Si to other known interstitial impurity centers. In Fig. 8, such a comparison of our D center with several known impurity centers is given, where the structure of the other centers was obtained by electron spin resonance measurements. A {110} plane of Si is shown in Fig. 8 where the cross-hatched Si atoms all lie within a given plane, the open circles correspond to Si atoms above and below that plane, and the H and T refer to hexagonal and tetrahedral interstitial sites, respectively. A striking similarity is seen between the D location and the structures for the carbon pair,²⁴ the boron interstitial,²⁵ and the aluminum pair.²⁶ All of these are located along $\langle 111 \rangle$ directions in the Si lattice in

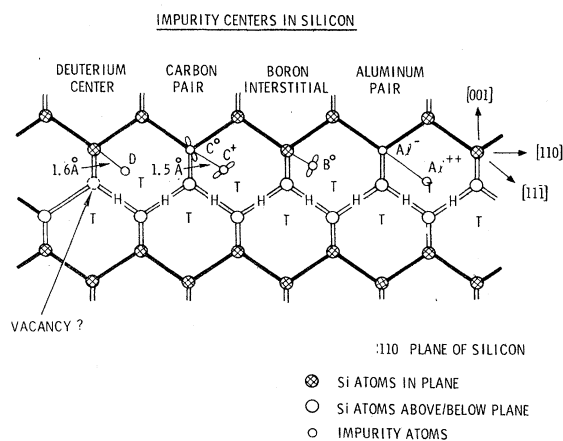


FIG. 8. Schematic of {110} plane in Si showing several identified interstitial impurity centers.

the antibond direction and have bond lengths which range from $\approx 1.5 \text{ \AA}$ for the C-C pair to nearly the tetrahedral site ($\approx 2.3 \text{ \AA}$) for the Al-Al pair distance. The C-C distance is quite similar to the 1.6 \AA we find for the Si-D distance. Also, most of these other impurities are known to have small distortions off the exact $\langle 111 \rangle$ direction. Because of the high D concentrations of several tenths of atomic percent for these studies relative to any impurities in the Si as well as the lack of any observed difference between intrinsic, or 1- and 10- Ω cm P- and B-doped Si, we conclude that the D center reported here is not associated with another impurity in Si.

While the D location is identified in the present experimental measurements, the nature of the surrounding lattice cannot be determined, and thus the possible association of Si vacancies or interstitials cannot be eliminated. However, by analogy with the other known impurity centers in Si, we point out that an adjacent vacancy or interstitial complex may not be required for this center to be stable.

A further consideration for the possible existence of a chemical bond without the presence of defects is given by the calculations of Appelbaum *et al.*¹² which predict such bonding on Si surfaces. Another consideration is the case of amorphous Si where the observed hydrogen concentration can exceed that observed for dangling bonds. Much of the prevailing opinion on the nature of hydrogen in amorphous silicon is that the hydrogen enters the Si lattice by saturating dangling bonds.¹ However, it is unreasonable to view the hydrogen as simply saturating dangling bonds in α -Si because of the relatively high hydrogen concentrations^{1, 2, 6, 27} (order of 1–50 at. %) which are incorporated relative to the smaller number of dangling bonds as measured by electron-spin resonance.²⁸ Thus, it is extremely important to resolve this question as to whether the D center occurs primarily by bonding to dangling Si bonds or can bond directly into the fully coordinated Si lattice.

In conclusion, the present results give the first experimental measurement of the structure of the hydrogen impurity center in Si. A single, relatively simple site is found and the D is located $\approx 1.6 \text{ \AA}$ along $\langle 111 \rangle$ directions from a Si site in the antibond direction. There is an indication that a small distortion ($\approx 0.1 \text{ \AA}$) transverse to this direction is present. No existing theoretical calculations presently predict this site, although relatively little theoretical work has been carried out on hydrogen in bulk Si. The present results should provide a basis for future theoretical work which is necessary to resolve the nature of hydrogen in silicon, both for crystalline and amorphous Si.

While these and other studies indicate the very strongly chemical and covalent bonding nature of hydrogen in the Si lattice, the present results cannot resolve the question of whether the D simply saturates dangling bonds or can be bonded directly into a fully coordinated Si lattice. It is important to resolve this question as to whether bond saturation or chemisorptionlike models are valid, both for our understanding of crystalline Si defects and

our understanding of the nature of amorphous Si.

ACKNOWLEDGMENTS

Experimental assistance by G. Harper and technical discussions with H. J. Stein and R. R. Rye are gratefully acknowledged. This work was supported by the U. S. Department of Energy, Contract No. AT(29-1)789.

-
- ¹See, for example, A. L. Robinson, *Science* **197**, 851 (1977); H. Fritzsche, C. C. Tsai, and P. Persons, *Solid State Technol.* **21**, 55 (1978).
- ²H. J. Stein and H. A. R. Wegener, *J. Electrochem. Soc.* **124**, 908 (1977).
- ³P. J. Zanzucchi, C. R. Wronski, and D. E. Carlson, *J. Appl. Phys.* **48**, 5227 (1977).
- ⁴S. M. Hu, in *Atomic Diffusion in Semiconductors*, edited by D. Shaw (Plenum, New York, 1973), p. 217.
- ⁵H. J. Stein, *J. Electron. Mater.* **4**, 159 (1975).
- ⁶M. H. Brodsky, M. A. Frisch, J. F. Ziegler, and W. A. Lanford, *Appl. Phys. Lett.* **30**, 561 (1977).
- ⁷W. K. Chu, R. H. Kastl, R. F. Lever, S. Mader, and B. J. Masters, *Phys. Rev. B* **16**, 3851 (1977).
- ⁸E. Ligeon and A. Guivarch, *Radiat. Eff.* **27**, 129 (1976).
- ⁹D. M. Gruen, R. Varma, and R. B. Wright, *J. Chem. Phys.* **64**, 5000 (1976).
- ¹⁰B. von Roedern, L. Ley, and M. Cardona, *Phys. Rev. Lett.* **39**, 1576 (1977).
- ¹¹P. B. Johnson, *Radiat. Eff.* **32**, 159 (1977).
- ¹²J. A. Appelbaum, D. R. Hamann, and K. H. Tasso, *Phys. Rev. Lett.* **39**, 1487 (1977).
- ¹³K. M. Ho, M. L. Cohen, and M. Schluter, *Phys. Rev. B* **15**, 3888 (1977).
- ¹⁴V. A. Singh, C. Weigel, J. W. Corbett, and L. M. Roth, *Phys. Status Solidi* **81**, 637 (1977).
- ¹⁵J. L. Yarnell, R. H. Lovberg, and W. R. Stratton, *Phys. Rev.* **90**, 292 (1953).
- ¹⁶S. T. Picraux, in *New Uses of Ion Accelerators*, edited by J. F. Ziegler (Plenum, New York, 1975), p. 229.
- ¹⁷J. A. Ellison and S. T. Picraux, *Phys. Rev. B* **18**, 1028 (1978).
- ¹⁸D. K. Brice, *Ion Implantation Range and Energy Deposition* (Plenum, New York, 1975), Vol. 1 and private communication.
- ¹⁹D. A. Thompson, J. E. Robinson, and R. S. Walker, *Radiat. Eff.* **32**, 169 (1977).
- ²⁰G. J. Janz and Y. Mikawa, *Chem. Soc. Jpn. Bull.* **34**, 1495 (1961).
- ²¹V. A. Singh (private communication).
- ²²See, for example, T. Sakurai, and H. D. Hagstrum, *Phys. Rev. B* **14**, 1593 (1976).
- ²³K. C. Pandey, T. Sakurai, and H. D. Hagstrum, *Phys. Rev. Lett.* **35**, 1728 (1975).
- ²⁴K. L. Brower, *Phys. Rev. B* **9**, 2607 (1974).
- ²⁵G. D. Watkins, *Phys. Rev. B* **12**, 5824 (1975).
- ²⁶G. D. Watkins, *IEEE Trans. NS-16*, 13 (1969).
- ²⁷M. H. Brodsky, *Extended Abst. Electrochem. Soc.* **77-2**, 793 (1977).
- ²⁸K. L. Brower and W. Beezhold, *J. Appl. Phys.* **43**, 3499 (1972).